



Homozygous indel mutation in *CDH11* as the probable cause of Elsahy–Waters syndrome

Ekim Z. Taskiran¹  | Beren Karaosmanoglu^{1,2} | Can Koşukcu¹ |
Özlem A. Doğan³ | Hande Taylan-Şekeroğlu⁴ | Pelin Ö. Şimşek-Kiper³  |
Eda G. Utine³ | Koray Boduroğlu³ | Mehmet Alikışıfoğlu¹

¹ Faculty of Medicine, Department of Medical Genetics, Hacettepe University, Ankara, Turkey

² Department of Stem Cell Sciences, Hacettepe University, Institute of Health Sciences, Ankara, Turkey

³ Faculty of Medicine, Department of Pediatric Genetics, Hacettepe University, Ankara, Turkey

⁴ Faculty of Medicine, Department of Ophthalmology, Hacettepe University, Ankara, Turkey

Correspondence

Ekim Z. Taskiran, Hacettepe University, Faculty of Medicine, Department of Medical Genetics, Ankara, Turkey.
Email: eztaskiran@hacettepe.edu.tr; ekimtaskiran@gmail.com

Funding information

Hacettepe University Turkey, Grant number: TAY-2015-7335

Two sisters from a consanguineous couple were seen in genetics department for facial dysmorphic features and glaucoma. They both had broad foreheads, hypertelorism, megalocorneas, thick eyebrows with synophrys, flat malar regions, broad and bulbous noses, and mild prognathism. Both had glaucoma, younger one also had cataracts and phthisis bulbi. Other findings included bilateral partial cutaneous syndactyly of 2nd and 3rd fingers, history of impacted teeth with dentigerous cyst in the elder one, and intellectual disability (mild and borderline). The sisters were considered to have Elsahy–Waters syndrome. In order to elucidate the underlying molecular cause, sisters and their healthy parents were genotyped by SNP arrays, followed by homozygosity mapping. Homozygous regions were further analyzed by exome sequencing in one affected individual. A homozygous indel variant segregating with the condition was detected in *CDH11* (c.1116_1117delinsGATCATCAG, p.(Ile372MetfsTer9)), which was then validated by using Sanger sequencing. *CDH11* encodes cadherin 11 (osteo-cadherin) that regulates cell–cell adhesion, cell polarization and migration, as well as osteogenic differentiation. Further experiments revealed that *CDH11* expression was decreased in patient-derived fibroblasts as compared to the heterozygous parent and another healthy donor. Immunostaining showed absence of the protein expression in patient fibroblasts. In addition, cell proliferation rate was slow and osteogenic differentiation potential was delayed. We consider that this study reveals loss-of-function mutations in *CDH11* as a probable cause of this phenotype. Next generation sequencing in further patients would both prove this gene as causative, and finely delineate this clinical spectrum further contributing in identification of other possibly involved gene(s).

KEYWORDS

CDH11, Elsahy–Waters syndrome, exome sequencing, osteo-cadherin

1 | INTRODUCTION

Elsahy–Waters syndrome was first described in siblings from a consanguineous couple in 1971, who had underdeveloped maxilla,

mandibular prognathism (relative or absolute), dental cysts, broad nasal bridge, hypertelorism, bifid uvula or partial cleft plate, pectus excavatum, fused cervical spinous processes, penoscrotal hypospadias, Schmorl nodes, and intellectual disability (ID)

(El-Sahy & Waters, 1971). This condition was later reported by a few authors (Shafai, Watters, & Pena, 1982; Wedgwood, Curran, Lavelle, & Trott, 1983; Witkop, 1975). Patients in two additional reports were considered to bear the same condition afterwards (Balci, Kayikcioglu, & Dagli, 1998; Reed, Shokeir, & Macpherson, 1975). Inheritance pattern is either X-linked, considering that all previous patients were males, or autosomal recessive considering both the original report and a more recent report in 2010 (Castori et al., 2010).

Acro-fronto-facio-nasal dysostosis (AFFND) is another rare malformation syndrome, characterized by ID and occasional genitourinary anomalies in addition to distinctive facial and skeletal anomalies. Craniofacial features include brachycephaly with wide anterior fontanel, prominent forehead with low frontal and occipital hairlines, flat malar region, hypertelorism, broad and bifid nasal tip with a broad philtrum, cleft upper lip, and highly-arched palate, prognathism, and small ears with prominent helices (Richieri-Costa, Colletto, Gollop, & Masiero, 1985). Eye anomalies including bilateral ptosis, coloboma of the upper lids, cataracts, congenital glaucoma, and iris atrophy have been reported (Chaabouni et al., 2008; Guion-Almeida & Richieri-Costa, 2003; Richieri-Costa, Guion-Almeida, & Pagnan, 1992). Skeletal features include syndactyly of fingers 3–4, small toes 3–5, and other structural anomalies of feet, with occasional fibular hypoplasia and short stature. Hypospadias, with or without cleft glans, and bifid scrotum were reported (Chaabouni et al., 2008; Naguib, 1988; Teebi, 1992). The disorder is autosomal recessively inherited.

Two sisters, born to their healthy first-cousin parents, were seen in genetics department for facial dysmorphic features, glaucoma, and mild ID. Based on their clinical features, this condition was considered to be consistent with El-Sahy–Waters syndrome, or less likely, AFFND. By means of “Hacettepe Exome Project,” which was started in July, 2015, at Hacettepe University in Ankara, Turkey, we aimed to search for the unknown genetic cause underlying this seemingly Mendelian phenotype. Herein, we report on the molecular findings in this family, including homozygosity mapping followed by exome sequencing, and studies on protein expression in fibroblasts. A homozygous indel variant in *CDH11* has been detected as the probable molecular cause of the condition, and this was supported by loss of function of the gene, demonstrated in fibroblasts of the elder sister.

2 | MATERIALS AND METHODS

Genomic DNAs were extracted from peripheral blood of the patients and/or their family members, using the standard protocols, after the receipt of the informed consent. Skin samples from two of the participants (the mother and the elder sister) were obtained by punch biopsy of the thigh. The study protocol was approved by Hacettepe University Ethics Committee (GO 15-530/25).

2.1 | Homozygosity mapping and exome sequencing

Genome-wide SNP analyses were performed by using Affymetrix 250 K SNP arrays according to manufacturer's recommendations. SNP

arrays were scanned on an Affymetrix GeneChip® Scanner 3000 7G (Santa Clara, CA). Vigenos Software (Hemosoft, Ankara, Turkey) was then used for homozygosity mapping (Kayserili et al., 2009).

Sequencing libraries were prepared from genomic DNA using the Ion AmpliSeq™ Exome RDY kit, that allows for amplifications by ultra-high multiplex PCR of the great majority of the Consensus Coding Sequences. The ~56 Mb target region includes >97% of the coding RefSeq exons and portions of flanking regions. Emulsion PCR was performed on Ion OneTouch™ 2 system using the Ion PI Template OT2 200 Kit, according to the manufacturer's instructions. Ion sphere particles (ISP) were enriched using the One Touch™ ES module. Then, ISPs were loaded on Ion PI chips and sequenced by using Ion Proton Semiconductor Sequencer (Thermo Fisher Scientific, Waltham, MA).

The Torrent Mapping Alignment Program (TMAP) was used for the alignment of the data to the human reference genome (hg19/GRCh37). Raw sequence file was processed by using Torrent Suite v5.0.5, for the generation of mapped reads, analysis of the coverage, and variant calling. Variants with a less than 5X coverage for SNVs (Single Nucleotide Variants) and 10X for INDELS were excluded for further analysis. Phred Quality Scores were specified as Q15 for SNVs and Q20 for INDEL variants. All variants passed the quality score filters were annotated with the Ion Reporter™ server (<https://ionreporter.thermofisher.com/ir/>).

Variants were further verified by Sanger sequencing by using BigDye Terminator v.3.1 Cycle Sequencing Kit and reaction products were applied onto ABI 3130 genetic analyzer (Thermo Fisher Scientific).

2.2 | Expression analysis of *CDH11* in dermal fibroblasts

Fibroblasts from skin biopsies, were grown in cell culture flasks in 60% DMEM-LG (Biochrom, Berlin, Germany), 40% MCDB 201 medium (Sigma-Aldrich, St Louis, MO), with 10% heat inactivated fetal bovine serum, 2 mM L-glutamine, and 1% Pen/Strep. Cells are incubated at 37°C and 5% CO₂. For further studies, passage 3 cells were used.

Total RNA was isolated from fibroblasts using TRIzol reagent (Invitrogen, Carlsbad, CA) according to manufacturer's protocol. cDNA was synthesized using Proto Script II First Strand cDNA Synthesis Kit (New England Biolabs, Ipswich, MA) according to the manufacturer's instructions. Quantitative real time PCR was performed with PowerUp™ SYBR Green Master Mix (Thermo Fisher Scientific) by using ViiA™ 7 Real-Time PCR System (Thermo Fisher Scientific). mRNA expression level was calculated relative to the ACTB by using delta delta Ct method. For allelic quantitation allele specific primers were used in order to compare wild-type and mutant alleles in heterozygous parent (I–2). Primer sequences are available upon request.

2.3 | Immunofluorescent staining

Fibroblasts were seeded on cover-glasses placed in a well of a six-well cell culture plates. Medium was removed and cells washed with PBS. Cells were incubated in a blocking solution (5% FBS in

PBS) at room temperature for 60 min. Afterwards, they were incubated in the primary anti-human CDH11 antibody (Catalog #: 368710, BioLegend, San Diego, CA), which was diluted 1:50 in blocking solution, at room temperature for 120 min and washed with the blocking solution. Cells were fixed with 3.7% paraformaldehyde at room temperature for 10 min and washed three times with PBS. Then, cells were incubated with secondary goat anti-mouse antibody (Catalog #: A-11031, Thermo Fisher Scientific) which was diluted 1:500 in blocking solution, at room temperature for 120 min and washed three times with PBS. Cells were counter-stained with DAPI at room temperature for 1 min and mounted with ProLong Gold antifade reagent (Invitrogen). Slides were visualized with Leica DMI 6000 B (Wetzlar, Germany) microscope.

2.4 | Analysis of cell proliferation and differentiation

Cell index (CI) impedance measurements were performed by using xCELLigence RTCA-SP system (ACEA Biosciences, San Diego, CA) according to the manufacturer's instructions. All the samples were seeded in triplicate and monitored every 60 min for 10 days.

StemPro Osteogenic Differentiation kit (Thermo Fisher Scientific) was used for osteogenic induction. After 21 days cells were fixed with 3.7% paraformaldehyde, stained with Alizarin Red S and visualized with Olympus CKX41 inverted microscope (Tokyo, Japan).

3 | RESULTS

3.1 | Clinical features

Two sisters (Figures 1a and 1b), born to first-cousin parents, were examined at the genetics department for their facial dysmorphic features, ID, and ocular problems.

The elder one (II-1, Figures 1a and 2) was born to the 19-year-old mother at 36th gestational week, with a birth weight of 2,750 g, birth length 47 cm, and head circumference (HC) 32 cm. No significant prenatal, natal, or neonatal problems were encountered. She had hypertelorism and was referred once again at 4^{9/12} years, prior to nasoplasty. Past history revealed mild developmental delay; with head and neck control at 6 months, independent walking, and speech at around 2.5 years of age. Physical examination revealed broad forehead, thick eyebrows with synophrys, hypertelorism and strabismus, mild malar flattening with a broad and bulbous nose, wide alae nasi, a broad philtrum, mild prognathism, malocclusion, and a high palate. She had bilateral partial mild cutaneous syndactyly of the fingers, particularly prominent between 2nd and 3rd fingers (Figure 2). Height was then 97 cm (3rd centile) and HC was 51 cm (50th centile). She had history of dental aids and surgery for several impacted teeth and extra teeth, as well as residual cysts and dentigerous cysts. Vertebral X-rays ruled out presence of any vertebral anomalies and Robinow syndrome. 3D (3-dimensional) cranial CT (computerized tomography) revealed hypertelorism. Follow-up examinations revealed normal HC, height (25th–50th

centiles), and weight (75th–90th centiles). Metabolic screening revealed no abnormality. Hearing was normal in both BAER test and audiological testing. Echocardiography, abdominal ultrasonography, orbital and cranial MRI, and chromosome analysis were all normal. A later skeletal survey revealed fusion between C2 and C3 cervical vertebrae (Figure 3). Psychometric assessment confirmed mild ID. She had a friendly personality with no deficits in social interaction. Her normal education was supported by an additional special education program. Figure 2 presents her facial appearance, hands and feet at the age of 18.

Complete ophthalmological examination was carried out at 16 years of age. Her best corrected visual acuity was 20/32 (with -1.25 to -3.50 axis 180) in the right eye and 20/32 (with -1.25 to -4.50 axis 180) in the left eye. Anterior segment evaluation revealed no abnormality except long globes (axial length was 26.38 mm in the right eye and 27.90 mm in the left eye). In the primary position she had a large angle exodeviation. Fundus examination showed bilateral increased cup/disc ratio (Figures 1c and 1d). The patient was started on topical antiglaucomatous medication to control bilateral high intraocular pressure.

The younger sister was first evaluated at 8 years of age (Figures 1b and 4). She was born to the 22-year-old mother at term with a birth weight of 3,200 g and a birth height of 52 cm. No prenatal, natal, or neonatal problems were encountered. Past history revealed that she was operated multiple times for bilateral glaucoma, first one at 8 months of age. She had only 10% visual acuity on the left eye, reportedly secondary to postoperative ocular infection. Initial development was grossly normal; sitting with support at 6 months, unaided walking at 15–16 months, and speech at 1st birthday. After 3 years of age she received special education, as she then had mild developmental delay with visual problems. Psychometric assessment revealed borderline ID. Further investigations revealed normal hearing, cardiac anatomy, abdominal sonographic exam, audiological tests, and chromosome analysis. At 8 years of age, height was 130 cm (75th–90th centiles), HC was 51.5 cm (50th centile), and weight 41.5 kg (>97th centile). She also had hypertelorism, thick eyebrows, broad nose with a bifid tip, wide philtrum, malocclusion due to maxillary retrusion and mandibular protrusion, high palate, and bilateral partial cutaneous syndactyly of fingers, particularly prominent in between 2nd and 3rd fingers (Figure 4). She had a widows peak and there was an incision scar over the bulbous nasal tip, secondary to a nevus excision. On follow-up, she weighed at 90th–97th centiles and her height remained at 25th–75th centiles. Like her sister, she was operated for multiple impacted teeth, even though no pathology reports were available. Skeletal survey yielded no vertebral pathology, but confirmed underdeveloped maxilla and mandibular malocclusion. She also had a friendly personality with no problems in social interaction. Figure 4 presents her facial appearance, hands and feet at the age of 14.

Complete ophthalmological examination was performed at 12 years of age. On ophthalmological evaluation, she had no light perception bilaterally. The biomicroscopy showed megalocornea, corneal cloudiness, peripheral iridectomy, and cataract in the right

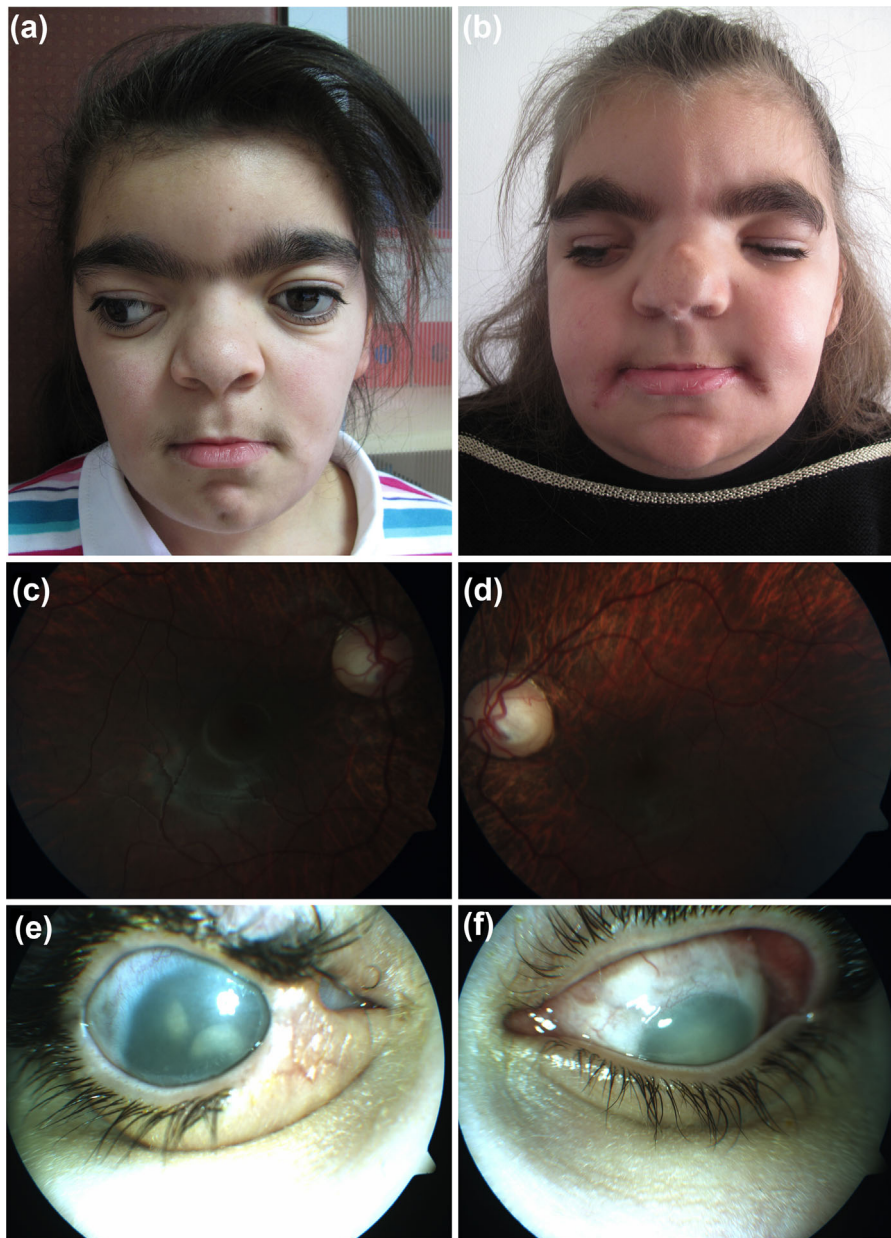


FIGURE 1 The facial photography of the (a) elder and (b) younger sister. Both sisters had thick eyebrows with synophrys, hypertelorism, exophthalmos, bilateral megalocorneas, underdeveloped maxilla, short and flat noses, wide alae nasi, long philtrums, thin upper lip vermillion, and thick lower lips. The younger one on the right had an incision scar over her bulbous nasal dorsum from a previous nevus excision. Fundus imaging of (c) the right eye and (d) the left eye of the first patient shows large and pale optic disc and optic disc cupping, prominent choroidal vessels, and tigroid retina appearance. Biomicroscopic view of the second patient: (e) The right eye has megalocornea, corneal cloudiness, peripheral iridectomy, and cataract. Medial tarsorrhaphy can be seen next to the medial canthus. (f) Severe corneal opacity limits the visualization of the anterior segment details in the left eye. [Color figure can be viewed at wileyonlinelibrary.com]

eye whereas it was impossible to perform detailed anterior segment evaluation in the left eye due to severe corneal opacity (Figures 1e and 1f). Both eyes were phthisical on ocular ultrasonography.

3.2 | Identification of disease-causing gene

Two healthy parents and affected siblings were genotyped using 250K-SNP array followed by homozygosity mapping using VIGENOS (Hemosoft). This analysis revealed five uninterrupted homozygous

regions in chromosomes 3, 4, 11, 16, and 17 (Supplementary Table S1). Parents were heterozygous in these regions, which (totally ~80 Mb) contain ~680 known and predicted RefSeq genes. Then, we tried to identify disease causing variants by using exome sequencing in one affected individual (II-2).

The following prioritization scheme was used to narrow down pathogenic variants. First, high quality variants registered in the dbSNP138 with a minor allele frequency of >1% were excluded. Then, synonymous substitutions and non-coding variants were filtered out. A



FIGURE 2 Facial appearance, views of hands and feet in the elder sister. The patient has a broad forehead, broad nose with bulbous nasal tip, proptosis, hypertelorism, and exodeviation of the eyes. Note presence of bilateral partial skin syndactyly in between fingers, most prominent between fingers 2 and 3. The patient also has bilateral hallux valgus. [Color figure can be viewed at wileyonlinelibrary.com]

total of 27 variants within the five different homozygous intervals were identified and five of them were not found in in-house exome variant database ($n = 252$ unrelated individuals) (Supplementary Table S1). Four of these variants were non-synonymous substitutions and one of them was not found in ExAC database (CNGB1 p.Gln208Arg). Mutations in CNGB1 cause retinitis pigmentosa (Bareil

et al., 2001), however, this variant is poorly conserved in evolution and it is less likely to be pathogenic (Supplementary Table S2).

The fifth variant in the critical intervals was an indel variant in *CDH11* (c.1116_1117delinsGATCATCAG). The variant segregating with the disease was validated with Sanger sequencing in all family members (Figures 5a and 5b).

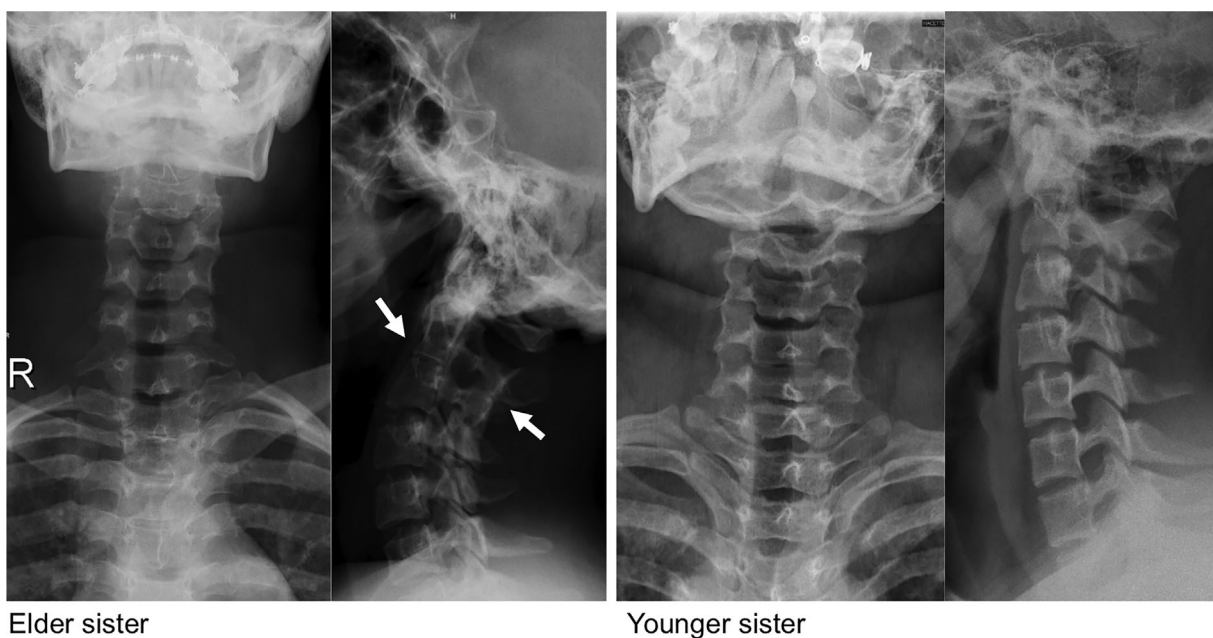


FIGURE 3 Fusion between cervical vertebrae C2–C3 (elder sister). Younger sister had normal vertebrae



FIGURE 4 Facial appearance, views of hands and feet in the younger sister. The patient has a broad forehead, broad nose with bifid nasal tip with an operation scar, hypertelorism, and narrow vertical palpebral aperture. Both eyes are enophthalmic and affected by glaucoma. Note presence of bilateral partial skin syndactyly in between fingers, most prominent between fingers 2 and 3. There is bilateral hallux valgus. [Color figure can be viewed at wileyonlinelibrary.com]

3.3 | Expression analysis of *CDH11* in dermal fibroblasts

The indel variant in *CDH11* (c.1116_1117delinsGATCATCAG, p.(Ile372MetfsTer9)) was predicted to cause a premature stop codon, which could lead to Nonsense Mediated Decay (NMD). Quantitative PCR analysis showed that *CDH11* expression was decreased in patient fibroblasts, as compared to the heterozygous parent (I-2) and the healthy donor (Figure 5c). Then, allele specific quantitation analysis in heterozygous parent (I-2) was performed and this data also confirmed that mutant allele was partially, but not totally, degraded by NMD (Figure 5d). The *CDH11* transcripts that were not degraded by NMD, lacked many critical protein domains including transmembrane domain, cadherin domains 4–6 and intracellular domain, due to the frameshift variant (Figure 5e). Immunostaining using anti-*CDH11* antibody showed that there was no protein expression in patient-derived fibroblasts (Figure 5f), ultimately leading to the conclusion that this indel variant caused complete loss of function of *CDH11*.

3.4 | Analysis of cell proliferation and osteogenic differentiation

Cell proliferation was monitored real-time using the xCELLigence for 10 days, in order to compare the patient's cells (II-1) proliferation rate with the heterozygous parent (I-2) and the healthy individual. The

doubling time was 75.07 (± 10.18) hr for the affected individual, 56.87 (± 7.38) hr for her mother, and 38.30 (± 3.84) hr for the healthy individual, showing that the cells from the patient had the slowest division rate (Figure 5g). As a result of the osteogenic differentiation process for 21 days of the fibroblasts from both affected individual and healthy individual, the osteogenic differentiation was found to be delayed in patients' cells (Supplementary Figure S1a-f). In addition to these, it is observed that the cellular morphology of the affected individual's fibroblasts was different from the healthy individual; it had more rounded shape possibly due to the loss of cell polarity (Supplementary Figures S1g and S1h).

4 | DISCUSSION

A homozygous loss-of-function mutation in *CDH11* was detected for the first time as a probable cause of the craniofacial phenotype in two sisters.

The most likely clinical diagnosis was considered as Elshahy–Waters syndrome in this sibling pair. This condition consists of underdeveloped maxilla, mandibular prognathism, dental cysts, hypertelorism, proptosis, broad nasal bridge, midface retrusion, bifid uvula or partial cleft plate, pectus excavatum, fused cervical spinous processes, penoscrotal hypospadias, Schmorl nodes and ID (El-Sahy & Waters, 1971). Dental anomalies like radicular dentin hypoplasia with consequent obliterated pulp chambers, apical translucent “cysts” and

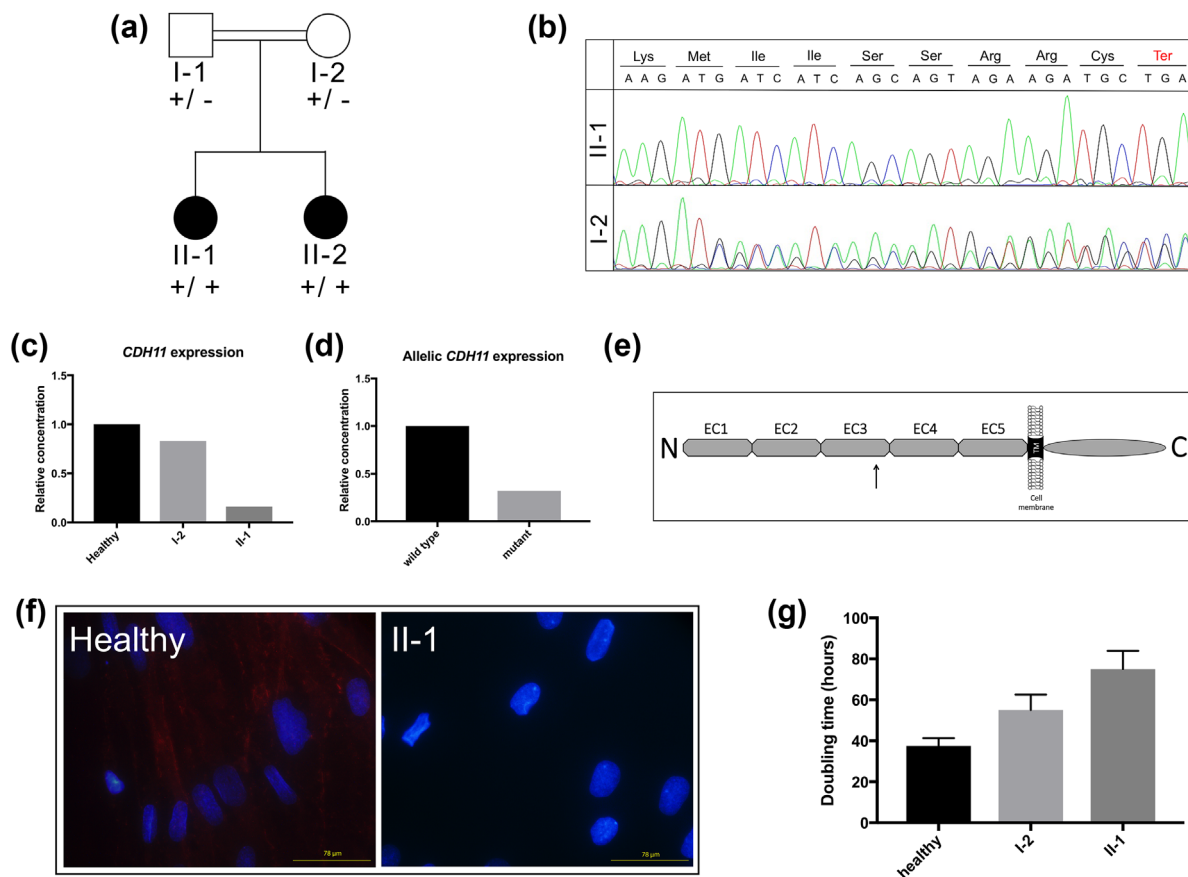


FIGURE 5 (a) Pedigree of the family. Square indicates male and circles indicate females. Solid symbols indicate affected individuals. Double-horizontal bars indicate consanguinity. (b) Sanger sequence electropherograms of the *CDH11* variant (c.1116_1117delinsGATCATCAG). The upper chromatogram reports the homozygous variant in one affected individual (II-1). The lower chromatogram shows the heterozygous variant in one of the parents (I-2). Codons and the corresponding amino acids are displayed above the chromatograms. (c) Relative quantitation of *CDH11* transcripts in fibroblasts from the healthy individual, a heterozygous parent (I-2), and the homozygous affected individual (II-1). (d) The allelic expression of *CDH11* was quantified by real-time PCR in fibroblasts from a heterozygous parent (I-2). (e) The schematic representation of the cadherin 11 protein. Mutation site is indicated by the arrow. EC, extracellular cadherin domains; TM, transmembrane domain; N and C represents amino and carboxy terminals of the protein respectively. (f) Immunofluorescent staining against *CDH11* in fibroblasts from the healthy individual (left) and affected individual (II-1, right). Cells were stained for nucleus (blue), and *CDH11* (red) by using anti-*CDH11* antibody. (g) The doubling time of the fibroblasts from the healthy individual, a heterozygous parent (I-2) and the affected individual (II-1), respectively, according to the 10-day long xCELLigence assay. [Color figure can be viewed at wileyonlinelibrary.com]

early loss of teeth may also be present (Castori et al., 2010). Facial appearance of the present sisters, history of impacted teeth, and dentigerous cysts, vertebral fusion, as well as borderline ID are suggestive of this condition.

Differential diagnosis includes AFFND, which in original description included two types, probably the spectral variations of a single condition. Type I (OMIM 201180) consisted of short stature, hypertelorism, broad and bifid nasal tip, cleft lip and/or palate, postaxial camptobrachypolysyndactyly, other skeletal anomalies and ID (Richieri-Costa et al., 1985), whereas the later described type II (OMIM 239710) consisted of facial midline defects, polysyndactyly, and genitourinary anomalies, but not ID (Richieri-Costa, Montagnoli, & Kamiya, 1989). Only a few patients with AFFND have been reported after the first description (Balci et al., 1998; Chaabouni et al., 2008; Guion-Almeida & Richieri-Costa, 2003; Naguib, 1988; Prontera et al., 2011; Teebi, 1992). All reported patients had ear anomalies, long philtrums, and syndactyly,

whereas two brothers also had upper lid colobomas (Balci et al., 1998), and one patient had glaucoma (Chaabouni et al., 2008). Facial appearance in this sibling pair, presence of ID, acral findings, and glaucoma in both sisters may be more consistent with AFFND. Absence of genitourinary anomalies excludes neither of the conditions as these are occasional anomalies in both conditions and previous patients with anomalies were all males. Based on past medical history, borderline ID in our patients may be partially secondary to early onset of visual problems, particularly in the younger sister.

Table 1 presents a comparison of the features in two sisters with AFFND and Elshahy-Waters syndrome. Presence of different opinions on previous patients with overlapping features may be supportive of a clinical spectrum which includes both conditions (Balci et al., 1998; Castori et al., 2010). As no next generation data from the previous patients were reported, genetic testing in new patients with these two conditions would be expected to elucidate the clinical confusion.

TABLE 1 A comparison of manifestations in AFFND and EWS with the present sisters

Manifestations	AFFND	EWS	Elder sister	Younger sister
Parental consanguinity	+	+	+	+
Normal birth weight and length	+	+	+	+
Normal head circumference	+	+	+	+
Normal growth parameters	+	+	+	+
Intellectual disability	+	+	Mild	Borderline
Brachycephaly	+	+	+	+
Asymmetric face	-	+	-	-
Broad/prominent forehead	+	-	+	+
Bitemporal narrowing	-	+	-	-
Widows peak	+	-	-	+
Thick eyebrows	-	+	+	+
Synophrys	-	+	+	+
Hypertelorism	+	+	+	+
Strabismus	+	+	+	+
Proptosis	+	+	+	+
Glaucoma	+	-	+	+
Cataracts	+	-	-	+
Midface retrusion	-	+	-	+
Flat malar region	+	-	+	+
Broad nasal tip	+	+	+	+
Bifid nasal tip	+	-	-	+
Low hanging columella	-	+	+	+
Thin upper vermillion	-	+	+	+
Prognathism/malocclusion	+	+	-	+
High palate	+	+	+	+
Cleft palate	+	+	-	-
Dental cysts	-	+	+	-
Impacted teeth	-	+	+	+
Skin syndactyly of fingers	+	-	+	+
Cervical vertebral fusion	-	+	+	-
Scoliosis	+	+	-	-
Pectus excavatum	+	+	-	-
Genitourinary anomalies	+	+	-	-

AFFND, Acro-fronto-facio-nasal dysostosis; EWS, Elshah-Waters syndrome.

The novel homozygous indel variant caused complete loss-of-function of *CDH11*. Mutant transcripts were mostly degraded and the predicted truncated protein was undetectable in fibroblasts of one of the affected individual (II-1). Cadherin 11, also called osteo-cadherin, is a member of cadherins that function in various developmental processes as cell adhesion receptors (Halbleib & Nelson, 2006). Cadherin 11 regulates cell-cell adhesions, cell polarization, and migration, as well as the osteogenic differentiation (Di Benedetto et al., 2010; Langhe et al., 2016; Marie et al., 2014; Mbalaviele, Shin, & Civitelli, 2006; Okazaki et al., 1994). In our study, decreased cell proliferation and delayed osteogenic differentiation

potential were shown in patient's cells. During normal osteogenic differentiation, a rapid cell proliferation takes place at the early stages (Kulterer et al., 2007), however, fibroblasts of the affected individual proliferated slowly in our osteogenic differentiation assay. At the end of the process, there was a significant delay in differentiation, confirming a loss-of-function in *CDH11*, as normal osteogenic differentiation requires expression of *CDH11* (Alimperti & Andreadis, 2015; Mbalaviele et al., 2006). Additionally, *CDH11* plays an important role in extracellular matrix synthesis through regulation of collagen and elastin synthesis (Row, Liu, Alimperti, Agarwal, & Andreadis, 2016). It is also expressed in cortical neurons

and has been shown to control cell migration during cortical development (Schulte et al., 2013).

To understand the exact function of *Cdh11*, Kawaguchi's group introduced a mice model, where they showed that cadherin-11 null mutant mice had normal external appearance like a wild-type mice, however, they had reduction in bone density at the femoral metaphyses, had some cranial malformations like round shaped skull, had decrease in diploë of calvaria, reduction in bone density that causes cranial defects (Kawaguchi et al., 2001). In addition, Manabe's group, created a *Cdh11*-deficient mice model and showed that these mice have behavioral defects such as showing less anxiety or fear related responses (Manabe et al., 2000). Because there is high sequence homology between human and mice, the effect of loss-of-function in cadherin-11 would expected to be similar. Human phenotype of *CDH11* mutation was reported very recently in one study (Anazi et al., 2017). Homozygous loss of function variant c.999 +1G>T was reported to cause ID with associated dysmorphic features. Although no photographs of the proband were available, the described phenotype appears consistent with the present sisters. The proband had a wide nasal bridge with hypertelorism and proptosis, as well as malar flattening and anteverted nares, had dental problems including delayed eruption of teeth, agenesis of incisors, and digital skeletal features, including shortening of all phalanges of the fingers. Delayed fine motor development and ID were present. Besides, the patient had synophrys and abnormality of the eyebrows, thin upper lip vermillion, and a pointed chin. Even though photographs are not available from this patient, description of facial features, in association with both dental and digital skeletal anomalies, supports presence of an overlapping clinical spectrum.

We consider that our study reveals homozygous loss-of-function mutation in *CDH11* as a probable molecular cause of this clinical spectrum. There might be additional causative genes as well, as this clinical condition may be one phenotype in a broader spectrum of similar phenotypes. Next generation sequencing in further patients would both prove this gene as causative, and finely delineate this clinical spectrum further contributing in identification of other possibly involved gene(s).

ACKNOWLEDGMENTS


We thank family members for their participation. We are grateful to Prof. Nurten A. Akarsu from the Department of Medical Genetics at Hacettepe University, for carrying out homozygosity mapping. This work was supported by Hacettepe University (Grant Number: TAY-2015-7335).

CONFLICTS OF INTEREST

The authors declare that they have no conflict of interest.

ORCID

Ekim Z. Taskiran  <http://orcid.org/0000-0001-6040-6625>

Pelin Ö. Şimşek-Kiper  <http://orcid.org/0000-0001-7244-7766>

REFERENCES

- Alimperti, S., & Andreadis, S. T. (2015). CDH2 and CDH11 act as regulators of stem cell fate decisions. *Stem Cell Research*, 14, 270–282.
- Anazi, S., Maddirevula, S., Faqih, E., Alsedairy, H., Alzahrani, F., Shamseldin, H. E., . . . Alkuraya, F. S. (2017). Clinical genomics expands the morbid genome of intellectual disability and offers a high diagnostic yield. *Molecular Psychiatry*, 22, 615–624.
- Balci, S., Kayikcioglu, A., & Dagli, A. S. (1998). Two brothers with hypospadias, hypertelorism, upper lid coloboma and mixed type hearing loss: A new syndrome. *Clinical Genetics*, 54, 440–442.
- Bareil, C., Hamel, C. P., Delague, V., Arnaud, B., Demaille, J., & Claustres, M. (2001). Segregation of a mutation in CNGB1 encoding the beta-subunit of the rod cGMP-gated channel in a family with autosomal recessive retinitis pigmentosa. *Human Genetics*, 108, 328–334.
- Castori, M., Cascone, P., Valiante, M., Laino, L., Iannetti, G., Hennekam, R. C. M., & Grammatico, P. (2010). Elshah-Waters syndrome: Evidence for autosomal recessive inheritance. *American Journal of Medical Genetics Part A*, 152A(1), 2810–2815.
- Chaabouni, M., Maazoul, F., Ben Hamida, A., Berhouma, M., Marrakchi, Z., & Chaabouni, H. (2008). Autosomal recessive acro-fronto-facio-nasal dysostosis associated with genitourinary anomalies: A third case report. *American Journal of Medical Genetics Part A*, 146A, 1825–1827.
- Di Benedetto, A., Watkins, M., Grimston, S., Salazar, V., Donsante, C., Mbalaviele, G., . . . Civitelli, R. (2010). N-cadherin and cadherin 11 modulate postnatal bone growth and osteoblast differentiation by distinct mechanisms. *Journal of Cell Science*, 123, 2640–2648.
- El-Sahy, N. I., & Waters, W. R. (1971). The branchio-skeleto-genital syndrome. A new hereditary syndrome. *Plastic and Reconstructive Surgery*, 48, 542–550.
- Guion-Almeida, M. L., & Richieri-Costa, A. (2003). Acrofrontofacionasal dysostosis: Report of the third Brazilian family. *American Journal of Medical Genetics Part A*, 119A, 238–241.
- Halbleib, J. M., & Nelson, W. J. (2006). Cadherins in development: Cell adhesion, sorting, and tissue morphogenesis. *Genes & Development*, 20, 3199–3214.
- Kawaguchi, J., Azuma, Y., Hoshi, K., Kii, I., Takeshita, S., Ohta, T., . . . Kudo, A. (2001). Targeted disruption of cadherin-11 leads to a reduction in bone density in calvaria and long bone metaphyses. *Journal of Bone and Mineral Research*, 16, 1265–1271.
- Kayserili, H., Uz, E., Niessen, C., Vargel, I., Alanay, Y., Tuncbilek, G., . . . Akarsu, N. A. (2009). ALX4 dysfunction disrupts craniofacial and epidermal development. *Human Molecular Genetics*, 18, 4357–4366.
- Kulterer, B., Friedl, G., Jandrositz, A., Sanchez-Cabo, F., Prokesch, A., Paar, C., . . . Trajanoski, Z. (2007). Gene expression profiling of human mesenchymal stem cells derived from bone marrow during expansion and osteoblast differentiation. *BMC Genomics*, 8, 70.
- Langhe, R. P., Gudzenko, T., Bachmann, M., Becker, S. F., Gonnermann, C., Winter, C., . . . Kashef, J. (2016). Cadherin-11 localizes to focal adhesions and promotes cell-substrate adhesion. *Nature Communications*, 7, 10909.
- Manabe, T., Togashi, H., Uchida, N., Suzuki, S. C., Hayakawa, Y., Yamamoto, M., . . . Chisaka, O. (2000). Loss of cadherin-11 adhesion receptor enhances plastic changes in hippocampal synapses and modifies behavioral responses. *Molecular and Cellular Neuroscience*, 15, 534–546.
- Marie, P. J., Haÿ, E., Modrowski, D., Revollo, L., Mbalaviele, G., & Civitelli, R. (2014). Cadherin-mediated cell-cell adhesion and signaling in the skeleton. *Calcified Tissue International*, 94, 46–54.
- Mbalaviele, G., Shin, C. S., & Civitelli, R. (2006). Cell-cell adhesion and signaling through cadherins: Connecting bone cells in their microenvironment. *Journal of Bone and Mineral Research*, 21, 1821–1827.

- Naguib, K. K. (1988). Hypertelorism, proptosis, ptosis, polysyndactyly, hypospadias and normal height in 3 sibs: A new syndrome? *American Journal of Medical Genetics*, 29, 35–41.
- Okazaki, M., Takeshita, S., Kawai, S., Kikuno, R., Tsujimura, A., Kudo, A., & Amann, E. (1994). Molecular cloning and characterization of OB-cadherin, a new member of cadherin family expressed in osteoblasts. *The Journal of Biological Chemistry*, 269, 12092–12098.
- Prontera, P., Urciuoli, R., Siliquini, S., Macone, S., Stangoni, G., Donti, E., . . . Belcastro, V. (2011). Acrofrontofacionasal dysostosis 1 in two sisters of Indian origin. *American Journal of Medical Genetics Part A*, 155A, 3125–3127.
- Reed, M. H., Shokeir, M. H., & Macpherson, R. I. (1975). The hypertelorism-hypo-spadias syndrome. *Journal of the Canadian Association Radiologists*, 26, 240–248.
- Richieri-Costa, A., Colletto, G. M. D. D., Gollop, T. R., & Masiero, D. (1985). A previously undescribed autosomal recessive multiple congenital anomalies/mental retardation (MCA/MR) syndrome with fronto-nasal dysostosis, cleft lip/palate, limb hypoplasia, and postaxial polysyndactyly: Acro-fronto-facio-nasal dysostosis syndrome. *American Journal of Medical Genetics*, 20, 631–638.
- Richieri-Costa, A., Montagnoli, L., & Kamiya, T. Y. (1989). Autosomal recessive acro-fronto-facio-nasal dysostosis associated with genitourinary anomalies. *American Journal of Medical Genetics*, 33, 121–124.
- Richieri-Costa, A., Guion-Almeida, M. L., & Pagnan, N. A. B. (1992). Acro-fronto-facio-nasal dysostosis: Report of a new Brazilian family. *American Journal of Medical Genetics*, 44, 800–802.
- Row, S., Liu, Y., Alimperti, S., Agarwal, S. K., & Andreadis, S. T. (2016). Cadherin-11 is a novel regulator of extracellular matrix synthesis and tissue mechanics. *Journal of Cell Science*, 129, 2950–2961.
- Schulte, J. D., Srikanth, M., Das, S., Zhang, J., Lathia, J. D., Yin, L., . . . Chenn, A. (2013). Cadherin-11 regulates motility in normal cortical neural precursors and glioblastoma. *PLoS ONE*, 8, e70962.
- Shafai, J., Watters, G. V., & Pena, S. D. (1982). The branchioskeletogenital syndrome. *Birth Defects Original Article Series*, 18, 193–196.
- Teebi, A. S. (1992). Naguib-Richieri-Costa syndrome: Hypertelorism, hypospadias, and polysyndactyly syndrome. *American Journal of Medical Genetics*, 44, 115–116.
- Wedgwood, D. L., Curran, J. B., Lavelle, C. L., & Trott, J. R. (1983). Cranio-facial and dental anomalies in the Branchio-Skeleto-Genital (BSG) syndrome with suggestions for more appropriate nomenclature. *British Journal of Oral Surgery*, 21, 94–102.
- Witkop, C. J., Jr. (1975). Hereditary defects of dentin. *Dental Clinics of North America*, 19, 25–45.

SUPPORTING INFORMATION

Additional Supporting Information may be found online in the supporting information tab for this article.

How to cite this article: Taskiran EZ, Karaosmanoglu B, Koşukcu C, et al. Homozygous indel mutation in *CDH11* as the probable cause of Elsahy-Waters syndrome. *Am J Med Genet Part A*. 2017;173A:3143–3152.
<https://doi.org/10.1002/ajmg.a.38495>